The Crystal Chemistry of Organic Metals. Composition, Structure, and Stability in the Tetrathiafulvalinium–Halide Systems

B. A. Scott,* S. J. La Placa, J. B. Torrance, B. D. Silverman, and B. Welber

Contribution from the IBM Thomas J. Watson Research Center, Yorktown Heights, New York 10505. *Received March 28, 1977*

Abstract: The results of crystal chemical studies of systems containing the organic π donor tetrathiafulvalene (TTF) with halogens (Z) are reported. In addition to the expected *isovalence* salts of the TTF mono- and dication, these systems also exhibit a series of segregated stack *mixed valence* salts of the type $(TTF)Z_\rho$, where $\rho < 1$. These compounds are comprised of separate TTF and Z sublattices where the ratio TTF:Z is nonintegral and defines the charge transfer ρ from the TTF stacks to the halide ion (which is fully charged). The mixed valence salts can be further classified into ordered or disordered halide sublattice types, with $0.7 \leq \rho(\text{ordered}) \leq 0.8$, and $\rho(\text{disordered}) < 0.7$. The ordered phases have small homogeneity ranges which were determined both by x-ray diffraction and chemical analysis techniques. The composition shift to lower halide content for the disordered phases suggests that the disorder is of the intrachain type. Using a simplified model structure, the unusual stoichiometries of the mixed valence phases are shown to be determined by the electrostatic Coulomb energies, which are maximized for ρ considerably less than one. Excellent agreement is obtained between calculated and observed mixed valence compositions. The importance of mixed valency to the general class of π-donor/acceptor salts, such as (TTF)(TCNQ), is also discussed within the context of this ionic model. Finally, from optical absorption and reflectivity studies of mixed valence (ρ = 0.59, 0.76) and fully ($\rho = 1$) charge transferred $(TTF)Br_\rho$ phases, an upper limit to the on-site Coulomb correlation energy, $U \approx 1.5$ eV at optical frequencies, is determined.

The high electrical conductivities displayed by organic charge transfer salts of the π donor tetrathiafulvalene (TTF, 2,2′-bi-1,3-dithiole[1]) and its derivatives[2] with organic π acceptors such as TCNQ[3] (tetracyano-*p*-quinodimethane) arise from a special feature of their crystal structures: electrons and holes are delocalized along segregated stacks of the cation donor and anion acceptor free radicals.[4] The presence of donor and acceptor stacks, both of which can potentially conduct, causes considerable complexities in the analysis of solid state properties of compounds such as (TTF)(TCNQ) and (TSeF)-(TCNQ).[5] Single donor (or acceptor) stack compounds should in principle provide simpler model systems in which an understanding can be gained of the electrical conductivities, optical properties,[6] and phase transitions in these pseudo-one-dimensional materials. Perhaps most importantly, through an examination of the simpler single stack compounds the fundamental questions can be investigated regarding structure and stability in these materials. For these reasons, we have studied the crystal chemistry and phase compositions of tetrathiafulvalinium–halide systems, in which compounds tend to form structures having single conducting donor stacks combined with simple, nonconducting halide anion chains.

In a recent publication we presented the crystal structure of the mixed-valence organic conductor $(TTF)Br_{0.71-0.76}$, and discussed its unusual composition in terms of qualitative Madelung energy arguments.[7] In the present work we have studied the TTF–Br, TTF–Cl, and TTF–I systems quite completely, and examine the interrelationship of structure, stability, and physical properties of the phases formed, which include a number of new ones not previously examined. Detailed electrical measurements have been reported on (TTF)Cl,[8] $(TTF)Br_n$ ($n \sim 0.7$), and several phases in the TTF–I system.[9,10] Transport measurements on $(TTF)-Br_{0.71-0.76}$, including thermoelectric power and its interpretation, will be presented separately.[11] In this paper our main goal is to determine the compositional phase diagrams of the TTF–halide systems and relate them to the important questions of structure and stability.

Experimental Section

Starting Materials. The TTF used in these studies was synthesized in accordance with published procedures[12] and purified by recrystallization and multiple gradient sublimation.[13] All other materials and solvents were AR grade and purified by distillation or nitrogen purging prior to use. Experiments were carried out under dry argon or nitrogen atmosphere.

Preparation of TTF–Halogen Salts. The primary method of investigating the phases formed in the TTF–halide systems consisted of titrating CCl_4 or CH_3CN solutions of TTF with standard solutions of Cl_2, Br_2 and I_2 in the same solvents. Typically, 1–2 mmol of TTF in 100–200 mL of solvent was oxidized. Denoting the fraction of TTF oxidized as ρ, experiments were performed at incremental values of ρ, taking care to measure the halogen concentration of the solutions prior to and following each experiment. Solid products were removed by filtration, washed and dried under vacuum, and analyzed chemically and by x-ray powder diffraction. In addition, the filtrate was tested for unreacted TTF or halogen. Carbon tetrachloride was found to be a good solvent for the oxidation of TTF because of the great insolubility of the salts formed; however, owing to its photochemical reaction with TTF,[14] experiments were carried out in the dark or under red light. As will be described, this reaction can be used to advantage, and was so applied to the preparation of several compositions difficult to obtain by any other method.

In addition to the above procedure, a number of experiments were carried out by an electrochemical method[15] which allowed precise control over the degree of oxidation ρ, prior to the addition of halogen (as halide ion). This method has the advantage of producing the equilibrium solid phase (or phase mixture) for a given ρ provided that the rate of reverse reaction is very small upon addition of halide ion to the oxidized solution. The reactions were carried out using 0.05–0.2 M tetraethylammonium perchlorate (TEAP) solutions in CH_3CN containing 1–2 mmol of TTF. A PAR 371 potentiostat was used in conjunction with a Koslow Model 541 coulometer. Potentials were measured against SCE, or 0.01 $AgNO_3$, in 0.1 M TEAP/CH_3CN solution, while bubbling under N_2, or while magnetically stirring in an argon drybox. Care was taken to ensure that any perchlorate salts of TTF remained dissolved during the electrolysis.

Single crystals of the various phases were grown by slow cooling of ethanol or acetonitrile solutions of materials prepared by the titration method, or by the U-tube technique[16] using electrochemically generated TTF^+/TTF^0 solutions of the desired value of ρ. In the latter method, one arm of the U-tube was filled with TTF^+/TTF^0 solution in acetonitrile (ClO_4^- counterion); the remaining arm contained the required tetraethylammonium halide salt in CH_3CN. The U-tubes were maintained at 30 °C in a thermostatically controlled (±0.05 °C) oil bath for periods of up to 2 months.

X-Ray Diffraction Measurements. Powder x-ray diffraction measurements were performed on all samples using a Philips diffracto-

Table I. Unit Cell Data for the TTF-Halides[a]

	Chlorides[b]	Bromides		Iodides[c]	
Dication salts	$(TTF)Cl_2$ $a = 13.56$ $c = 10.10$ $N = 8; I4_1/acd$	$(TTF)Br_2$ $a = 13.78$ $c = 10.56$ $N = 8; I4_1/acd$		Not obsd	
Monocation salts	(TTF)Cl $a = 11.073$ $b = 11.218$ $c = 13.95$ $N = 8; PbCa$	(TTF)Br $a = 11.242$ $b = 11.366$ $c = 14.143$ $N = 8; PbCa$		Not obsd	
Ordered mixed valence salts	$(TTF)Cl_{0.77}$ $a = 10.77$ $b = 3.56$ $c = 22.10$	$(TTF)Br_{0.76}$ sublattice: TTF $a = 15.617$ $b = 15.627$ $c = 3.572$ $\beta = 91.23°$	Br 17.368 15.623 4.538 116.01°	$(TTF)I_{0.72}$ sublattice: TTF 15.988 16.114 3.558 90.96°	I 8.19 16.11 4.871 102.82°
Disordered mixed valence salts	$(TTF)Cl_{0.68 \pm 0.02}$ $a = 11.12$ $c = 3.595$ Å	$(TTF)Br_{0.59 \pm 0.02}$ $a = 11.05$ $c = 3.562$		$(TTF)I_{0.69 \pm 0.02}$ $a = 11.34$ $c = 3.77$	

[a] In Å units, maximum standard deviation ±0.05%. N = number of formula units/cell. [b] Preliminary indexing of the $(TTF)Cl_{0.90}$ x-ray powder pattern is discussed in footnote 22. [c] The triiodide salt $(TTF)I_2$ observed but not included in this table (see General Discussion and ref 19a).

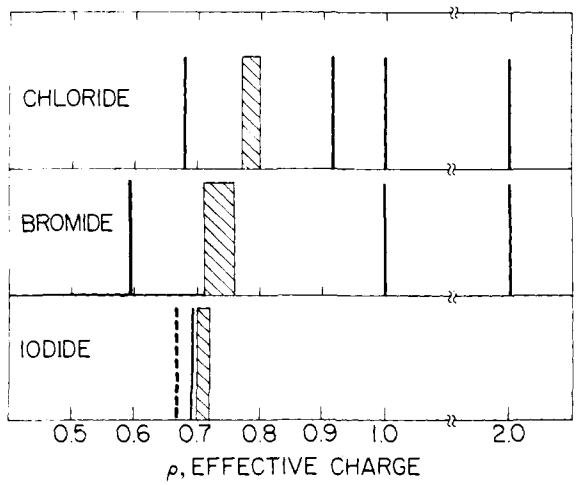

Figure 1. Phases observed in the (TTF)-halide(Z) systems plotted as $(TTF)Z_\rho$, where ρ is the halogen content defining the effective (or averaged) charge per cation site as discussed in the text. The dashed line corresponds to "$(TTF)I_2$" as explained in the General Discussion.

meter with Ni-filtered Cu Kα radiation and a graphite crystal monochromator at the receiving slit. These data were supplemented with measurements taken with a Guinier powder camera using a silicon internal standard. Crystal and molecular structures were determined using an Enraf-Nonius CAD4 single-crystal diffractometer, computer controlled by an IBM System 7. The details will be reported separately.[17]

Optical Measurements. Optical measurements[6b] were conducted on powder samples in KCl and KBr pellets, polycrystalline thin films, and single crystals, using several techniques. Absorption measurements were made on ≈1 wt % concentrations in pressed KCl or KBr disks using a Cary 14 spectrophotometer for the near-IR and visible spectra, and a Perkin-Elmer 301 for $\lambda > 2.5\mu$. To test the validity of the results obtained with the disks, polycrystalline films were prepared by sublimation onto c-axis sapphire and (100) NaCl substrates, and measured in the absorption mode. Finally, reflectance measurements were performed on single crystals using a special optical microspectrophotometric system.[18] This system permitted polarized measurements down to $\lambda = 1.8\mu$ on single crystals as small as 0.5 mm in length provided that they were smoothly faceted. The optical measurements will be discussed in more detail and compared to solution spectra elsewhere.[6b]

Experimental Results

Stoichiometry of Phases in the TTF–Halide Systems. Since the crystal chemistry of the TTF-Br system was initially found to be the simplest to understand,[7] much of the present work concentrated on the products of reaction of TTF and bromine, and their physical properties. Therefore, considerable discussion will center on this system, and results on the TTF-Cl and TTF-I systems will be compared directly to it.

The phases isolated in the three TTF-halogen systems are summarized diagramatically in Figure 1, and their crystallographic parameters are given in Table I. The observed phase compositions are delineated in terms of an effective cation charge parameter ρ, which is here defined by the results of chemical analysis of the *isolated, pure* phases, i.e., the halide content of their lattices. This parameter therefore provides a measure of degree of oxidation of the TTF chains in the compounds formed, or the degree of charge transfer *from* the donor stacks to the acceptors, which are fully charged. Summarizing the results briefly, we find two kinds of $(TTF)Z_\rho$ phases: the simple isovalence cation phases with $\rho = 1$ and 2, and the mixed valence segregated stack compounds where ρ is fractional and < 1. These latter compounds can be further divided into disordered and ordered halide sublattice phases, where we find $0.7 < \rho(\text{ordered}) < 0.8$ and $\rho(\text{disordered}) < 0.7$. Distinct homogeneity ranges were discovered[7] and determined for the ordered phases. Note that in all subsequent discussion we use "degree of oxidation" and "degree of charge transfer" interchangeably for the mixed valence phases. It is to be understood that "complete oxidation" or "fully charge transferred" refers to a system at $\rho = 1$, i.e., that consisting entirely of monocations.

Isovalence Compounds. Dication Salts. Insulating, yellow-orange crystals of $(TTF)Cl_2$ and $(TTF)Br_2$ can be prepared by direct oxidation in solution with a stoichiometric quantity of Cl_2 and Br_2. The insulating electrical properties observed are not surprising because TTF^{2+} is an even-electron cation whose highest lying bonding π MO is empty. $(TTF)Cl_2$ and $(TTF)Br_2$ are tetragonal and isomorphic, containing severely distorted (nonplanar) dications; i.e., the two halves of the molecule are rotated ~60° with respect to each other around the central C-C bond. The full structure will be published separately,[17] but the unit cell and space group data are given

in Table I. The stoichiometric reaction with I_2 yielded a mixture of phases, and attempts to electrochemically prepare $(TTF^{2+})(I^-)_2$ were unsuccessful, since I^- reduced the dication to the neutral molecule. The crystal structure of a compound of composition $(TTF)I_2$ was found by Johnson and co-workers[19] to contain the I_3^- anion, so that $\rho = 0.67$ (dashed line in Figure 1), as will be subsequently discussed.

Wudl has reported[19c] two additional iodide phases with stoichiometries $(TTF)_{24}I_{63}$ and $(TTF)_8I_{15}$. These may also contain I_3^- or higher polyiodide species, and have not been included in Figure 1 because their isolation was not attempted in the present study.

Monocation Salts. Oxidation of TTF using a stoichiometric quantity ($\rho = 1$) of Cl_2 or Br_2 in CCl_4 or CH_3CN solution invariably leads to a mixture of phases, the stoichiometries and amounts of which depend upon reaction conditions. Generally, slow titration of the stoichiometric quantity of bromine into the TTF solution led to a phase mixture containing the partially oxidized (mixed valence) TTF-subhalide nearest in composition to the 1:1 salt and the 1:2 dication salt $(TTF)Br_2$ (see Figure 1). Pure 1:1 salt could be prepared by very rapid addition of bromine to the TTF solution, but this method was not consistently reproducible, often resulting in a mixture of (TTF)Br with $(TTF)Br_{0.76}$ and $(TTF)Br_2$. Crystals of the 1:1 salt could be grown by slow cooling of ethanol solutions in which *single phase* 1:1 powders had been dissolved at the boiling point of the solvent; however, recrystallization of phase mixtures containing $(TTF)Br_{0.76}$ + $(TTF)Br_2$ whose gross compositions were 1:1 always led to crystals of the major, subhalide phase. We believe that this is due to the greater solubility of the subhalide phase, combined with a solution equilibrium favoring the presence of TTF^0 over the relatively long period (several days) of the crystal growth experiments. These factors result in a solution composition which is <1:1 in monocation:bromide ion, and thus the crystallization of the subhalide phase. Attempted synthesis of (TTF)Cl by reaction of TTF with Cl_2 in CCl_4 or CH_3CN led to even more complicated results, since in this system three subhalide phases occur at $\rho = 0.90$, 0.77-0.80, and 0.68. In the stoichiometric reaction ($\rho = 1$) all of these phases are obtained in mixture with (TTF)Cl and $(TTF)Cl_2$, the proportions of each depending upon the rapidity of Cl_2 addition. For these reasons, (TTF)Cl as well as (TTF)Br were prepared electrochemically[15] by completely oxidizing 0.005 M TTF solutions in CH_3CN to the monocation, and adding excess tetraethylammonium halide. The resulting solids gave 1:1 stoichiometries by chemical analysis and showed single phase x-ray diffraction patterns which could be indexed completely on the basis of the isomorphic orthorhombic unit cells shown in Table I. Crystals were grown from an electrochemically oxidized solution in a U-tube.

As shown in Figure 2, the orthorhombic unit cell of (TTF)Br contains eclipsed TTF^+ dimers, tilted ~24° with respect to the c axis, with an intradimer spacing of 3.34 Å. This separation is considerably shorter than the 3.57 Å found[7] in the eclipsed TTF stacks of the highly conducting mixed valence phase, $(TTF)Br_{0.71-0.76}$, which will be discussed subsequently. The dimers are interspersed with pairs of bromine ions with an interhalogen distance of 4.15 Å. The halide ions as well as the center of the TTF^+ molecules, shown in the a-axis bounded projection of Figure 2, lie nearly in the bc plane. The projected structure at $a/2$ can be simply visualized by displacing the unit cell contents by $b/2$. Thus, the structure of (TTF)Br exhibits nearly complete isolation of the $(TTF^+)_2$ dimers along the c axis, with only "weak" interchain contact of the ethylenic parts of the cation. (TTF)Cl is isomorphic with the unit cell parameters listed in Table I. As expected from this structure, (TTF)Br was found to exhibit a powder compaction conductivity $\sigma < 3 \times 10^{-4}$ $(\Omega\ cm)^{-1}$, and two probe conductivity

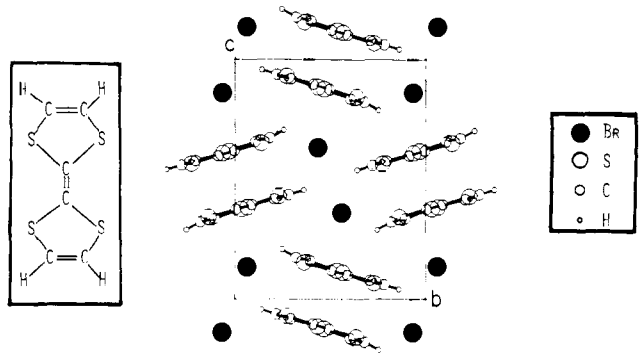

Figure 2. Bounded (a-axis) projection of the orthorhombic crystal structure of (TTF)Cl and (TTF)Br. The left insert shows the molecular formula of the TTF molecule.

measurements along b and c indicated that both σ_b, $\sigma_c < 10^{-6}$ $(\Omega\ cm)^{-1}$. We have found that electrical measurements on (TTF)Br powders are very sensitive to the presence of small amounts of highly conducting subhalide phase, and since it was very difficult to eliminate all traces of this phase even in the electrochemically prepared material, we may take the compaction result as an upper limit to the electrical conductivity of (TTF)Br. Thus, fully oxidized (i.e., completely charge-transferred) (TTF)Br and (TTF)Cl are essentially insulating in comparison with the mixed valence subhalide salts, whose conductivities are typically $\sigma \simeq 100$-500 $(\Omega\ cm)^{-1}$. It should be mentioned that the relatively high conductivity, $\sigma \sim 0.25$ $(\Omega\ cm)^{-1}$, originally reported by Wudl[8] for compactions of (TTF)Cl suggests that those samples, though "stoichiometric" by chemical analysis, were impure and contaminated by both the subhalide and superhalide phases shown in Figure 1 for this system.

Attempts to prepare (TTF)I by direct titration, or electrochemically, were unsuccessful. In the former case, a mixture containing primarily the subhalide $(TTF)I_{0.72}$ and other unidentified phases was obtained by the addition of a stoichiometric amount of I_2 to the TTF solution. This agrees with the results of Somoano and co-workers.[10] Moreover, the addition of I^- to solutions of electrochemically prepared monocation resulted in rapid, complete reduction of TTF^+ to TTF^0.

Mixed Valence Salts. Ordered Phases. By far the most interesting TTF-halide compounds are those with $\rho < 1$, for these are highly electrically conducting and necessarily exhibit mixed valence TTF sites. Figure 1 indicates the compositions of the mixed valence phases as determined by chemical and x-ray diffraction analysis of products obtained by direct reaction of the halogens with TTF in acetonitrile or carbon tetrachloride.

The prominent mixed valence TTF-halide is the composition $(TTF)Z_\rho$ with $0.7 < \rho < 0.8$, occurring for all of the halogens, Z. We have previously reported[7a] the two subcell structure and homogeneity range of $(TTF)Br_{0.71-0.76}$. The projection of this structure encompassing four of the monoclinic unit cells is shown in Figure 3. The basic structure consists of two separate, ordered, incommensurate, monoclinic sublattices for TTF and Br. Lattice parameters of both unmodulated sublattices are given in Table I for the composition $(TTF)Br_{0.76}$, which is the maximum limit in the homogeneity range of this compound. The structure contains an equal number of TTF and Br stacks running along the c axis. The unusual homogeneity range of this compound, in which the Br contents of the crystals vary, affects the Br-subcell dimensions, as shown in Figure 4. The TTF-subcell parameters remain essentially unchanged with composition. Since the reciprocal lattice a^* b^* nets for both ordered subcells are dimensionally identical and parallel, the chemical composition (and also the degree of oxidation of the TTF chains) must be $\rho = 3.57/c_{Br}$,

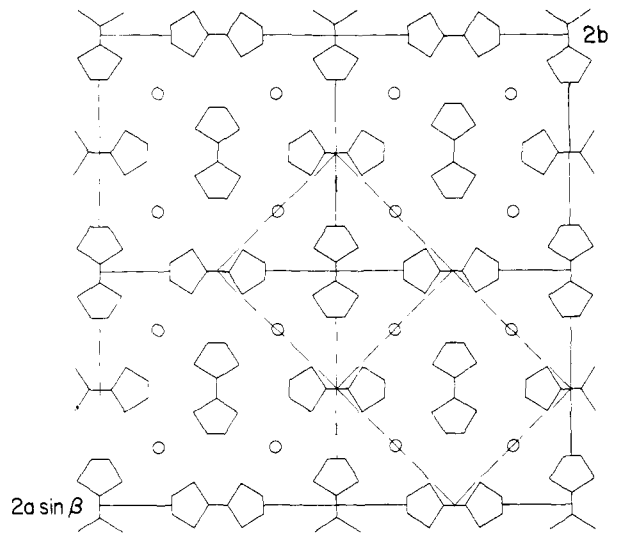

Figure 3. Projection parallel to the c-stacking axis of the crystal structures of all mixed valence $(TTF)Z_\rho$ phases ($\rho < 1$), with the exception of $(TTF)Cl_{0.90}$. The various unit cells and their symmetries are given in Table I. The largest dashed cell corresponds to that of orthorhombic $(TTF)Cl_{0.77\text{-}0.80}$.

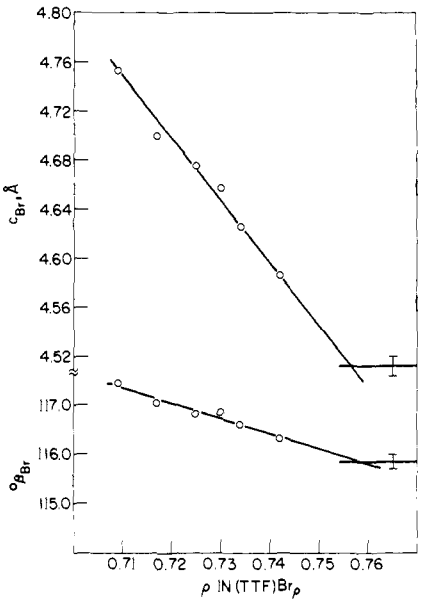

Figure 4. Variation of Br-subcell c parameter and monoclinic angle β as a function of chemical composition (effective cation charge) ρ in the *ordered*, mixed valence $(TTF)Br_\rho$ phases. The vertical bars define the range of each parameter observed in the two phase region above the upper boundary of the homogeneity range.

where c_{Br} is the composition-dependent Br sublattice c-axis spacing and 3.57 Å is the compositionally independent TTF sublattice c-axis spacing. Using this relationship, the x-ray determined homogeneity range would be ρ = 0.74-0.79, compared to the range ρ = 0.71-0.76 based upon the chemically analyzed compositions shown in Figure 4. Possible reasons for the discrepancy were previously discussed[7a] and will be examined again in a subsequent section. It should be pointed out that the vertical bars in Figure 4 define the range of each parameter observed in the two-phase region above the upper boundary of the homogeneity range. The lower boundary at ρ = 0.71 defines the point at which no further variation in parameters was observed in samples from TTF solutions oxidized to values of ρ as low as 0.3.

An elegant analysis of the three-dimensional modulated structure of a corresponding mixed valence iodide phase $(TTF)I_\rho$ (ρ = 0.7076) has been reported by Johnson et al.[19b] We have found $0.70 \leq \rho \leq 0.72$ for the homogeneity range of this phase, which is isomorphic with the bromide. The narrow range is based upon the chemical analysis of crystals grown from partially oxidized solutions whose compositions were adjusted to lie both above and below these limits. In Table I we have denoted the iodide-sublattice parameters on the basis of an A-centered subcell (space group $A2/m$) for comparison with the results of Johnson et al.:[19b] a_2 = 8.213, b_2 = 16.041, c_2 = 5.023 Å, and β_2 = 103.0°. These are in good agreement with our results for $(TTF)I_{0.72}$, except for the c_2 parameter. This difference clearly reflects the difference in composition between the two crystals: 0.7076 vs. 0.72.

The mixed valence chloride phase $(TTF)Cl_{0.77\text{-}0.80}$ is simply related to those just discussed for TTF-Br and TTF-I. It exhibits an x-ray diffraction pattern which can be completely indexed on the basis of the orthorhombic unit cell given in Table I. The stacking direction is now defined as the b axis. The relationship of this orthorhombic cell to that of the defect bromide and iodide phase is shown in Figure 3. Confirmation of the existence of a homogeneity range was obtained from long exposure single crystal oscillation photographs which revealed very weak incommensurate satellite reflections showing a chloride composition dependence. Thus, all of the highly conducting mixed valence compounds are structurally related, with the iodide and bromide salt isomorphic. In addition, all exhibit homogeneity ranges of a few percent within the ρ = 0.7-0.8 composition region. Their compositions directly and unambiguously define the extent of oxidation of the TTF chains, and therefore the "degree of charge transfer". This is because halogen with its large electron affinity is always crystallographically present as Z^-, with the exception of some of the iodide salts, as will be subsequently discussed.

Disordered Phases. In addition to the subhalide phases existing between ρ = 0.7 and 0.8, Figure 1 shows that all of the TTF-halide systems contain a second mixed-valence phase at a lower halide composition. The major characteristic of this phase is the complete disappearance of all halide sublattice x-ray reflections. The remaining reflections can be indexed on the basis of the tetragonal unit cell parameters given in Table I, i.e., the smaller tetragonal cell (dashed) shown in Figure 3: $a(\text{tet}) = a(\text{mono})/\sqrt{2}$; $c(\text{tet}) = c(\text{mono})$. These characteristics indicate that the halide subcells are disordered. Note that a composition shift to lower ρ always accompanies the disorder, with the exception of $(TTF)I_{0.69}$, where the small measured composition change relative to $(TTF)I_{0.70\text{-}0.72}$ is within the experimental error of the lower composition boundary of the ordered compound. However, like $(TTF)Br_{0.59}$ and $(TTF)Cl_{0.68}$, which show large composition shifts relative to their ordered phases ($\Delta\rho$ = 0.12 and 0.09, respectively), we believe that the actual degree of TTF oxidation in $(TTF)I_{0.69}$ is comparable to that in the bromide and chloride systems, although not directly revealed in a stoichiometry change. This is because the degree of charge transfer can be lowered in the iodide through the formation of I_3^- without a net composition shift:

$$2TTF^+ + 3I^- \rightarrow 2TTF^0 + I_3^-$$

Since this catenation process is far less favorable for Cl^- and Br^-, the charge transfer change upon disordering for the chloride and bromide is necessarily observed as a composition shift, while it need not be for the iodide (or the composition shift is marginal). Therefore, $\Delta\rho$ could be 0.1, or larger, for this phase. Since we do not know $\Delta\rho$, the disordered iodide is shown at the location of its *chemical* composition in Figure 1.

The observed composition shifts for the bromide and chloride phase upon disordering are evidence that the disorder is of the intrachain rather than interchain type. A composition shift would not be expected to accompany interchain disorder,

which involves unlocking the registry of the c-axis halide sublattice chains from cell to cell. Such disorder would still preserve the halide-halide spacing. On the other hand, simple lattice stability arguments, to be subsequently discussed, do suggest that intrachain disorder, in which the halide-halide spacing becomes irregular, can be expected to lower the charge transfer, and hence the halide composition, of the disordered phase.

General Discussion

With the exception of $(TTF)Cl_{0.68}$, we have found it generally difficult to routinely produce the disordered mixed valence phases in each system. Small crystals of $(TTF)Br_{0.59}$ have been prepared by slow cooling of saturated solutions chemically oxidized to $\rho \approx 0.5$, and adding a large excess of bromide ion. It could also be prepared by slowly heating the ordered $(TTF)Br_{0.71-0.76}$ phase to 120 °C under constant vacuum of 10^{-5} Torr. Flash evaporation of the ordered compound onto a cooled quartz substrate (0 °C) also produced disordered $(TTF)Br_{0.59}$. Thin films ~1000 Å thick were prepared in this manner for optical absorption measurements to be described in a subsequent section. The disordered chloride phase could be obtained as crystals from solution, most commonly as a mixture with the ordered orthorhombic form. Nevertheless, the disordered forms in each system could be routinely prepared as powders by photochemical oxidation of TTF in halocarbon solutions (such as CCl_4), carried out as we have previously outlined.[14] For reasons not completely understood, the electrochemical method was not consistently successful in producing the disordered phase. On the other hand, the ordered phases could be routinely prepared in this manner, or by direct titration with halogen followed by recrystallization. A discussion of the important solution equilibria governing the formation of the mixed valence phases will be published separately.[20]

Disordered tetragonal $(TTF)Cl_{0.68}$ appears to be identical with the disordered phase "$(TTF)Cl_{0.90}$" reported by Dahm et al.[21] with lattice constants a = 11.118 and c = 3.588 Å. These values are identical with ours for $(TTF)Cl_{0.68}$ (Table I). In the present study, we in fact observed a compound whose composition is close to that claimed for the disordered phase by Dahm and co-workers: $(TTF)Cl_{0.92 \pm 0.02}$ (Figure 1). Its x-ray powder pattern was clearly different and more complex[22] than that of $(TTF)Cl_{0.68}$. Since our samples consistently showed a composition within ±3% of ρ = 0.68 for the disordered phase, we believe that the composition claimed by Dahm and co-workers[21] is incorrect, as it is based entirely on the structural refinement and has not been verified by chemical analysis.[23] Unfortunately, crystals of $(TTF)Cl_{0.90}$ could not be obtained for structural analysis. However, additional evidence that ρ = 0.68 is the correct stoichiometry of the disordered form was obtained in x-ray diffraction experiments on single crystals of the ordered, orthorhombic compound. On exposure for ~100 h with Cu Kα radiation, crystals of the ordered $(TTF)Cl_{0.77}$ phase completely transform to a poor-quality crystal of the disordered tetragonal form. The simplest effect of the radiation would be disordering of the halide sublattice and subsequent loss of chlorine. In the unlikely event of an increase in chlorine content upon irradiation, exsolved TTF would appear as a second phase. No evidence for it was found following irradiation.

As previously mentioned, an interesting feature of the ordered mixed valence salts is that the ratio of the c axes of the TTF and Br sublattices should directly measure their compositions. This is because the cross-sectional unit cell areas perpendicular to the c axis are identical for the two cells. There is, however, a discrepancy for the bromide between the range measured by chemical analysis (Figure 4, ρ = 0.71-0.76) and that based on the ratio of c axes (ρ = 0.74-0.79). There is much less of a discrepancy for the iodide, where we find for the upper limit to the composition range ρ(analysis) = 0.72 vs. ρ(c-ratio) = 0.73. A possible explanation for the difference between calculated and observed bromide compositions may be the presence of small amounts of the disordered phase, with its lower value of ρ, in our samples of the ordered form. The disordered form would escape x-ray detection since its x-ray powder pattern is identical with that of the ordered compound, but with the halide sublattice reflections absent. If this were the case, it would explain the better agreement between ρ-(analysis) and ρ(c-ratio) for the iodide, which undergoes little, if any, change in composition upon disordering. On the other hand, $\Delta\rho$ is large for the bromide system, so that ~20 wt % of the disordered phase (ρ = 0.59) as an impurity in mixture with the ordered form could lower the bulk chemical analysis. We believe this to be a more likely source of the differences observed, although neglect of the periodic modulation of the TTF sublattice by the bromide sublattice, as previously discussed,[7a] still remains a possibility.

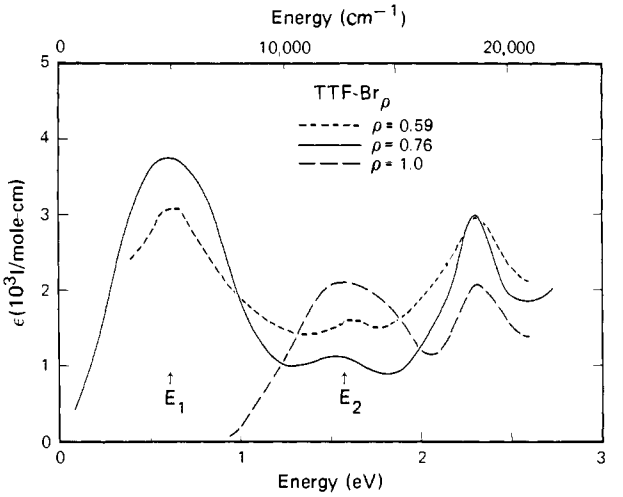

Figure 5. Infrared absorption spectra of $(TTF)Br_\rho$ compounds with ρ = 0.59, 0.76, and 1.0, showing the effect of the degree of oxidation. The spectra were taken on pelletized dispersions (1 wt % concentrations) of each compound in KBr or KCl matrices (ρ = 0.76, 1.0), or thin films (ρ = 0.59).

Electrical measurements to be reported separately[7a,11] indicate conductivity magnitudes consistent with organic "metallic"-like behavior ($\sigma \approx$ 100-500 $(\Omega\,cm)^{-1}$) for all the subhalide phases, although there might be small energy gaps present in the ordered bromide and iodide compounds[9-11] at room temperature. Single crystal measurements[9] have been carried out on $(TTF)I_2$. This compound contains disordered I_3^- stacks,[19a] and is thus more clearly written in the mixed valence formulation $(TTF^0)(TTF^+)_2(I_3^-)_2$. It is shown as ρ = 0.67 in the iodide system of Figure 1 (dashed line). Its conductivity is some five orders of magnitude lower than monoclinic $(TTF)I_{0.70-0.72}$. In contrast, our powder compaction conductivity comparisons between the ordered and disordered subhalide phases suggest very comparable room temperature values. Thus, if suitable crystals could be grown, an especially important study would be a comparison of the electrical behavior of the ordered vs. disordered subhalide phases.

IR Spectrum

The existence of a sequence of well-defined solid phases of different composition in the TTF-halide systems permits a direct examination of the effect of the degree of oxidation of the TTF chains upon the optical absorption spectra. The spectra[6b] are shown in Figure 5 for $(TTF)Br_\rho$ phases with ρ = 0.59 (sublimed film), 0.76 and 1.0 (dispersions in KBr and

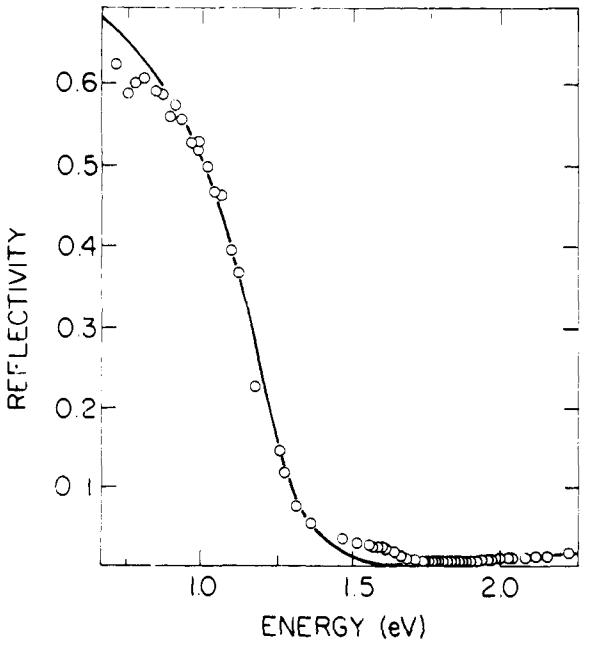

Figure 6. Normal incidence reflectivity spectrum for single crystal (TTF)$Br_{0.76}$. Light polarized along ⟨001⟩.

Table II. Dielectric Parameters[a] of the Drude and Lorentz Fits of Reflectivity Data for (TTF)$Br_{0.76}$ and (TTF)Br

(TTF)$Br_{0.76}$ (Figure 6); Drude Fit	
	$\epsilon = \epsilon_\infty - \dfrac{\omega_p^2}{\omega(\omega + i/\tau)}$
Best fit Parameters	$\epsilon = 2.4$
	$\omega_p = 1.93$ eV
	$\tau^{-1} = 0.26$ eV
(TTF)Br (Figure 7): Lorentz Fit	
	$\epsilon = \epsilon_\infty - \dfrac{\omega_p^2}{(\omega^2 - \omega_0^2) + i\omega\Gamma}$
Best fit Parameters	$\omega_p = 0.79$ eV
	$\omega_0 = 1.517$ eV
	$\Gamma = 0.071$ eV
	$\epsilon = 6.64$

[a] All units converted to electron volts. In the Lorentz fit, Γ is the half-width, ω_p the "plasma" frequency, and ϵ_∞ the high-frequency dielectric constant. The Drude fit is made assuming the fundamental oscillator frequency $\omega \rightarrow 0$, and τ is the electronic relaxation time.

KCl). The film absorption data were normalized to the 2.2 eV transition, which corresponds closely to one of the localized (intramolecular) excitations of TTF^+ in solution.[6b,24]

Both mixed valence phases of TTF-Br exhibit very similar near-IR spectra, with absorption peaks at $E_1 = 0.6$ and $E_2 = 1.55$-1.6 eV. On the other hand, only the higher transition at E_2 is observed in the fully oxidized (TTF)Br. Single crystal reflectivity measurements with light polarized parallel to the stacking axis, shown in Figures 6 and 7, also clearly reveal the difference between mixed valence ($\rho = 0.76$) and fully charge-transferred ($\rho = 1$) phases. The parameters of Drude and Lorentz fits to the reflectivity data for the respective phases are given in Table II. Note also that there is extra structure at ~1.6 eV in the reflectivity data of Figure 6, above and beyond that which can be ascribed to the excitations associated with the Drude fit. As discussed elsewhere,[6b] this structure is associated with the weaker E_2 transition shown in the absorption mode of Figure 5. For the fully oxidized $\rho = 1$ phase (Figure 7, Table II) the local oscillator frequency in the Lorentz fit gives $\omega_0 = 1.52$ eV, which is close to the value $E_2 = 1.55$ eV

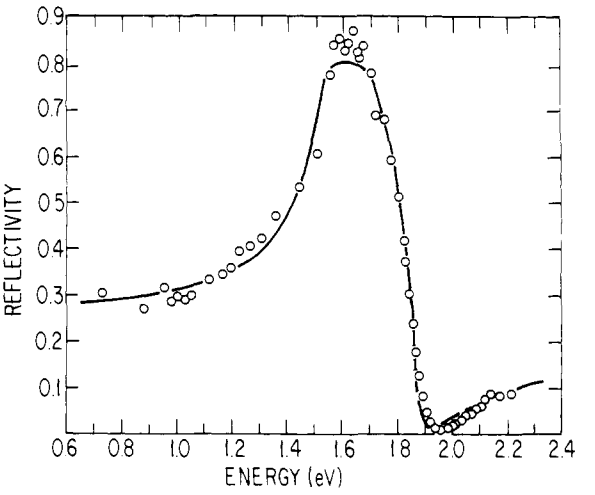

Figure 7. Reflectivity spectrum of (TTF)Br. Light incident on (111) face polarized with its major component along ⟨001⟩.

observed in the absorption data of Figure 5 for the $\rho = 1$ composition, and nearly identical with the energy at the "extra" reflectivity of Figure 6.

The optical properties of charge transfer salts of TCNQ have been previously described[6a,25] using a Hubbard-like model in which the lowest energy IR absorption is assigned to a mixed valence, intraband transition, and the higher energy IR absorption to interband excitations (isovalence) along the donor/acceptor stacks of these compounds. By comparison with these more complex, two-chain, TCNQ systems, we assign the spectra of Figure 5 for $\rho = 0.59$ and $\rho = 0.76$ to analogous transitions in these single stack compounds.[6b] Thus, the absorption centered at $E_1 = 0.6$ eV can be interpreted as an intervalence charge transfer transition of the type (TTF^0, TTF^+) → (TTF^+, TTF^0), and the band at $E_2 = 1.55$ eV, as an isovalence transition of the type (TTF^+, TTF^+) → (TTF^{2+}, TTF^0). Indeed, such assignments are entirely consistent with the results of Figures 5-7: first,both transitions are polarized along the stacks; also, both E_1 and E_2 transitions would be expected in the highly conducting subhalide compositions $\rho = 0.59$ and 0.76, but only the higher energy transition at E_2 should be observed in the $\rho = 1$ sample, since it contains only $(TTF^+)_2$ isolated dimers. We have previously related the transition at E_2 with the Coulomb intermolecular correlation energy, U, associated with the repulsion of two charges on a given molecule.[6a,25] Thus, as discussed in detail elsewhere,[6b] we estimate that $U \approx 1.5$ eV at near-IR frequencies.

For the highly conducting ordered mixed valence compound ($\rho = 0.76$), the observed (Figure 6, Table II) plasma frequency $\omega_p = 1.386$ eV is somewhat larger than the results obtained in the isomorphic iodide:[9b] $\omega_p = 1.15$ eV. In addition, based on the parameters of Table II, we extrapolate the optical conductivity to zero frequency: $\sigma = \omega_p^2\tau/4\pi \approx 200\ (\Omega\ \text{cm})^{-1}$, compared with sample dependent experimental values[7a,11] ranging from 200 to 500 $(\Omega\ \text{cm})^{-1}$.

Stabilization of the Mixed Valence State

In this section we discuss the factors which determine the unusual stoichiometry of the mixed valence halide salts discussed in the previous sections. We will show how the electrostatic binding energy of these ionic crystals favors a mixed valence structure, with calculated values of ρ in quantitative agreement with experiment. In addition, this picture is also able to account for the observed variations of ρ for different halides as well as for the ordered and disordered phases. We shall see, furthermore, that the unusual stoichiometry of these systems provides particularly clear and direct evidence of the important

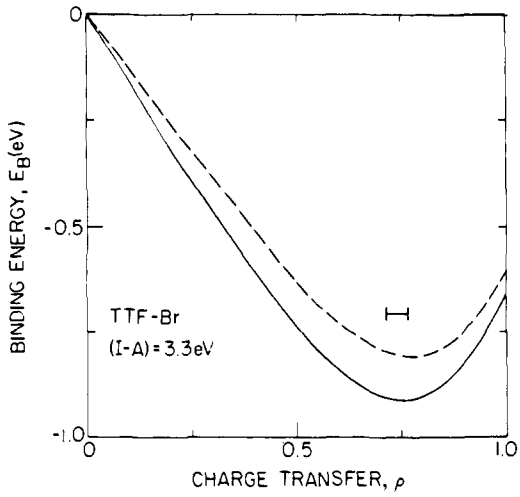

Figure 8. The binding energy of (TTF)Br_ρ as a function of composition ρ for the simplified structure defined in the text. Dashed line: without band energy E_t. Solid line: band energy included, assuming a bandwidth of 0.6 eV. The observed stoichiometry range is shown by the bars.

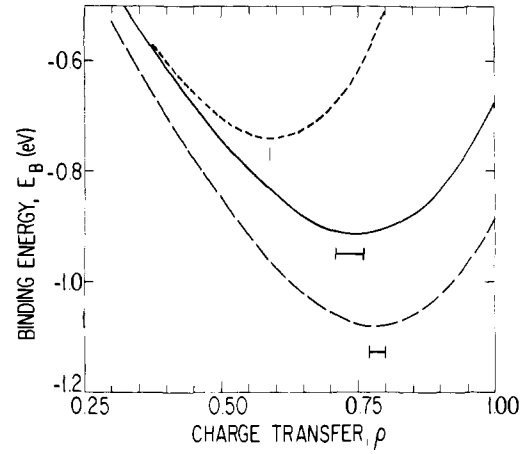

Figure 9. Calculations showing (a) binding energy of ordered (TTF)Cl_ρ as a function of composition, or degree of oxidation, ρ: long dashed curve and (b) the effect of disorder on the binding energy of the mixed valence bromide phases: solid curve, ordered compound; short dashed curve, disordered phase. Band energies have been included in the calculations. Bars indicated the observed composition ranges.

electronic property of mixed valence, which is more subtly manifested in other systems such as (TTF)(TCNQ).[6,26]

These calculations of the classical electrostatic, or Madelung, energy will be only briefly summarized below, since they are discussed in more detail elsewhere.[26] We assume a model structure for (TTF)Br_ρ which exists over the entire range $0 \leq \rho \leq 1$. For calculating the Madelung energy of this model, the TTF^0 molecules are neglected and the remaining TTF^+ and Br^- ions are assumed to lie in sheets parallel to the $ab(\sin\beta)$ plane, like those in Figure 3. These sheets of charge are separated from adjacent sheets by a variable spacing $z = z_0/\rho$, which is larger than (or equal to, for $\rho = 1$) the spacing $z_0 = 3.57$ Å between neighboring TTF molecules along the stack in (TTF)$Br_{0.76}$. The Madelung energy is calculated for a lattice of these sheets, spaced a distance z apart, and the dependence on ρ is simulated by varying z. Over the range $0.71 \leq \rho \leq 0.76$, this model structure is a good description of the Br^- ions in the observed structure of (TTF)Br_ρ, although the TTF molecules are not so accurately represented. For the molecular charge distribution over the TTF^+ molecules, the CNDO/2 charge densities of Metzger and Bloch[27] have have been used. Using the Ewald method,[28] the Madelung energy, $E_M{}^+(\rho)$, per TTF^+ ion was calculated. The *net electrostatic binding energy*, $E_B(\rho)$, normalized per TTF molecule (including both TTF^+ and TTF^0) is given by

$$E_B(\rho) = -\rho(|E_M{}^+(\rho)| - (I - A)) \qquad (1)$$

In this expression, the energy gained is the ionic Madelung binding energy, $\rho|E_M{}^+(\rho)|$, while the cost of partially ionizing the lattice is $\rho(I - A)$, where I is the ionization potential for TTF and A is the electron affinity of Br. Using the experimental values[29,30] of $I = 6.85$ eV (gas phase) and $A = 3.54$ eV, the results shown by the dashed line in Figure 8 were obtained. These results explicitly indicate that the mixed valence compositions with $\rho \approx 0.75$ are more binding than their hypothetical $\rho = 1$ analogues (i.e., $z = 3.57$ Å). This result can thus account for the observation of mixed valence subhalide salts, and is also consistent with our finding that the observed phase at $\rho = 1$ has adopted another structure (integrated stack, Figure 2).

A physical interpretation of the results in Figure 8 may be given in the following way: as Br^- is added and ρ increases, the binding energy per TTF molecule (including neutrals) initially increases as the percentage of ionized TTF^+ molecules increases. But as $\rho \rightarrow 1$ and the Br^-–Br^- spacing becomes shorter, the repulsion between like charges along the stacks begins to dominate, giving rise to a minimum in the electrostatic binding energy as a function of ρ. The kinetic (or covalent) energy, $E_t(\rho)$, associated with electronic delocalization along the stacks has also been included (assuming a value of 0.6 eV for the bandwidth) and added to the Madelung energy to give the solid line curve in Figure 8. The inclusion of the kinetic energy is seen to make a small, but important, contribution to the location of the minimum.[26]

These results can be readily extended to the ordered mixed valence chloride and iodide salts of TTF. Since the structures of these salts are very similar to the bromide, we shall assume that the most important difference between them in the electron affinities (~0.22 eV higher for Cl and ~0.28 eV lower for I, compared with Br[30]). Using these different values of A, we can calculate $E_B(\rho)$, as shown by the long dashed curve in Figure 9 for (TTF)Cl_ρ. Thus, we find the optimum calculated value of ρ to be ~0.78 for (TTF)Cl_ρ and ~0.70 for (TTF)I_ρ, compared to 0.77–0.80 and 0.70–0.72 determined experimentally (Figure 1).

We now attempt to understand the effect of halide disorder on the composition of the mixed valence phase. Let us imagine the ordered (TTF)$Br_{0.76}$ structure, for example, with the Br^- ions disordered along the stack. Qualitatively, the disordering of the Br^- ions would cost considerable electrostatic energy, since the latter is optimized for this value of ρ by an ordered stack. If the value of ρ were smaller, however, there might be more "room" for the ions to disorder without appreciable cost in Coulomb energy. More quantitatively, we can consider a sequence of identical charges, q_{n-1}, q_n, q_{n+1}, . . . , forming an ordered chain with a separation r between the charges. The repulsive Coulomb potential, V, at q_n due to the charges q_{n-1} and q_{n+1} is simply $2q/r$. If the chain is disordered by displacing each charge from its equilibrium position by a (variable) amount, z, the potential at q_n becomes

$$\bar{V} = q \int_0^\infty P(z) \left[\frac{1}{r+z} + \frac{1}{r-z}\right] dz \qquad (2)$$

where $P(z) = (1/r)\exp(-z/r)$ is the probability of finding the next charge as a function of z along the chain (see Appendix). Integrating (2) yields $\bar{V} = 1.3(2q/r)$; that is, the net effect of the disorder is to *increase* the effective Coulomb repulsion between like charges along the stack by a factor of ~1.3. This increased repulsion favors an increased spacing between the halide ions along the stack and hence a decreased value of ρ,

as observed. For the purpose of calculating $E_B(\rho)$, we may simulate the effects of this increased repulsion by representing the disordered structure by an ordered structure with a shorter lattice constant along the stack (shorter by the factor 1.3). Using this model for the disordered $(TTF)Br_\rho$ structure, the calculated $E_B(\rho)$ is shown by the short dashed curve in Figure 9. The optimum values of ρ calculated are ~0.59 and ~0.68 for the disordered bromide and chloride, respectively. In both cases, the magnitude of the net binding energy is not as large as in the ordered phases, as expected. Note that the calculation for the disordered $(TTF)Cl_\rho$ phase is not shown in Figure 9.

It should be recognized that other possibly important interactions have not been included in our Madelung calculations.[26,31,32] Nevertheless, the good agreement obtained using only classical electrostatic (and kinetic) interactions suggests that these are the most important ones for determining ρ, at least in the TTF-halide systems. Perhaps a more sensitive indication of the significance of this calculation is the good agreement with the trends in the other halide salts. Thus, $(TTF)Z_\rho$ with $\rho = 1$ would be too repulsive in a segregated stack structure and the electrostatic (and kinetic) binding is enhanced for a mixed valence, partly ionic stack of TTF molecules, with the Z^- ions uniformly spaced in separate, incommensurate sublattices. These calculations can therefore be of great help in understanding the stoichiometry of organic charge transfer salts.

As we have seen, the crystal binding energy is optimized for single organic stack structures such as the TTF subhalides by forming a mixed valence stack. In this case, the mixed valency is achieved by adopting a halide deficient structure. In the case of the two stack charge transfer salts of TCNQ, such deficiencies in the donor-acceptor stacks would be sterically unfavorable. The ability of TCNQ (like TTF) to exist as either neutral molecules or singly charged ions in a crystal permits the two stack systems to adopt mixed valence states on both donor and acceptor stacks to optimize E_B. In this case, the mixed valence state is achieved by incomplete transfer of charge from the donor to TCNQ. Indeed, the existence of neutral and negatively charged TCNQ in (TTF)(TCNQ) on the photoemission times scale has been claimed in ESCA measurements, where analysis of the observed splitting of the N(1s) core levels was used to estimate $\rho \approx 0.67$ for this salt.[33] Although this interpretation of the ESCA results has recently been questioned on several grounds,[34] it has now become clear on the basis of low-temperature diffuse x-ray[35] and neutron scattering[36] experiments that the degree of charge transfer in (TTF)(TCNQ) is in fact very close to this value: $\rho \simeq 0.59$. A summary of the controversy regarding the interpretation of the photoemission data has recently been published.[33c]

Thus, for the 1:1 salts of some strong π donors with TCNQ, size and steric considerations favor 1:1 stoichiometry, but the electrostatic energy favors a mixed valence state, obtained via incomplete charge transfer. Electrostatics is such an important factor that other TCNQ salts containing donors which can only assume a unipositive charge (e.g., the quaternary ammonium salt cations, quinolinium, the alkali metal cations, etc.) are forced to assume complex stoichiometries containing neutral TCNQ, in order to lower the intrastack repulsion. There are many examples of such phases, including $Cs_2(TCNQ)_3$ and $(Et_4N)(TCNQ)_2$, which have been reviewed in the crystallographic literature.[37] These points are discussed in detail elsewhere for the entire class of TCNQ salts.[26]

We strongly emphasize that the calculations shown in Figures 8 and 9 in no way suggest that the minima in electrostatic energy represent a calculation of lattice *stability*.[26] A recent investigation has examined the stability of a segregated stack in donor-acceptor complexes by *explicitly* treating an attractive metallic delocalization along the stack as well as the repulsive Coulomb interaction.[38]

Summary and Conclusions

Careful crystal chemical and phase studies of the TTF-halide systems have shown the existence of mixed valence donor-halide salts having segregated stack structures, in addition to the fully charge transferred $\rho = 1$ and 2 phases. The mixed valence phases occur with both ordered and disordered halide sublattices, and ρ(disordered) < ρ(ordered). The stability of the $\rho < 1$ mixed valence compounds was shown to be related directly to the greater Madelung binding of the subhalide compounds compared to their hypothetical, fully charge transferred ($\rho = 1$), segregated stack structures. Additionally, the near IR spectra of the $\rho = 0.58$, 0.76, and 1.0 compounds allow us to estimate the intramolecular Coulomb correlation energy, $U \approx 1.5$ eV. Finally, as discussed previously,[6a] mixed valency is of paramount importance to the attainment of high electrical conductivity in the entire class of segregated stack compounds. Not only does $\rho < 1$ stabilize E_M, but it also effectively avoids U BY PROVIDING= ON A TIME SCALE OF ORder of the reciprocal of the bandwidth, sites for electrons (or holes) to reside which are not already populated; e.g., $(TCNQ^-, TCNQ^0) \rightarrow (TCNQ^0, TCNQ^-)$. Thus, the electrostatic need for mixed valency creates a physically stable ground state in which there exist nearly optimum conditions for high electrical conductivity in these segregated stack, pseudo-one-dimensional, organic charge transfer salts.

Acknowledgments. We wish to thank R. Thomas, R. B. Braccini, and R. Linn for their technical assistance. We are also indebted to D. C. Green and F. B. Kaufman for their advice and help with the electrochemical preparatory technique, and to Mr. Green for growing crystals of the mono- and dibromide phases. R. A. Craven and P. E. Seiden provided the computer fits to the reflectivity data.

Appendix

Call $W(z)$ the probability of *not* finding another charge after moving a distance z from an arbitrary point along a one-dimensional chain. Then

$$W(z + y) = W(z)W(y)$$

and therefore

$$W(z) = e^{-z/r}$$

where r is the average distance between charges in the disordered chain. The probability of going a distance z without finding a charge, but then finding it in the next interval Δz, is

$$\lim_{\Delta z \to 0} W(z)(1 - W(z)) = e^{-z/r}(1 - e^{-z/r})$$

$$= e^{-z/r}(1 - 1 + (\Delta z/r) - \ldots)$$

$$\lim_{\Delta z \to dz} W(z)(1 - W(z)) = e^{-z/\lambda}dz/r = P(z)dz$$

where $P(z)$ is now the probability of finding a charge after moving a distance z.

References and Notes

(1) F. Wudl, G. M. Smith, and E. J. Hufnagel, *Chem. Commun.*, 1453 (1970).
(2) For a complete compilation of various TTF derivatives synthesized to date, and their TCNQ salts, see E. M. Engler, *Chemtech*, **6**, 274 (1976).
(3) (a) D. S. Acker, R. J. Harder, W. R. Hertler, W. Mahler, L. R. Melby, R. E. Benson, and W. E. Mochel, *J. Am. Chem. Soc.*, **82**, 6408 (1960); (b) D. S. Acker and W. R. Hertler, *ibid.*, **84**, 3370 (1962); (c) L. R. Melby, R. J. Harder, W. R. Hertler, W. Mahler, R. E. Benson, and W. E. Mochel, *ibid.*, **84**, 3374 (1962).
(4) T. J. Kistenmacher, T. E. Phillips, and D. O. Cowan, *Acta Crystallogr., Sect. B*, **30**, 763 (1974).
(5) Y. Tomkiewicz, A. R. Taranko, and J. B. Torrance, *Phys. Rev. Lett.*, **36**, 751 (1976).

(6) (a) J. B. Torrance, B. A. Scott, and F. B. Kaufman, *Solid State Commun.*, **17**, 1369 (1975); (b) J. B. Torrance, B. A. Scott, B. Welber, and F. B. Kaufman, to be published.
(7) (a) S. J. La Placa, P. W. R. Corfield, R. Thomas, and B. A. Scott, *Solid State Commun.*, **17**, 635 (1975); (b) B. A. Scott, J. B. Torrance, S. J. La Placa, P. Corfield, D. C. Green, and S. Etemad, *Bull. Am. Phys. Soc.*, **203**, 496 (1975); (c) S. J. La Placa, J. E. Weidenborner, B. A. Scott, and P. Corfield, *Ibid.*, **203**, 496 (1975).
(8) F. Wudl, D. Wobschall, and E. J. Hufnagel, *J. Am. Chem. Soc.*, **94**, 670 (1972).
(9) R. J. Warmack, T. A. Callcott, and C. R. Watson, *Phys. Rev. B*, **12**, 3336 (1975).
(10) R. B. Somoano, A. Gupta, V. Hadek, T. Datta, M. Jones, R. Deck, and A. M. Herman, *J. Chem. Phys.*, **63**, 4970 (1975).
(11) P. Chaikin, R. A. Craven, S. Etemad, and B. A. Scott, to be published.
(12) L. R. Melby, H. D. Hartzler, and W. A. Sheppard, *J. Org. Chem.*, **39**, 2456 (1974).
(13) A. R. McGhie, A. F. Garito, and A. J. Heeger, *J. Cryst. Growth*, **22**, 295 (1974).
(14) B. A. Scott, F. B. Kaufman, and E. M. Engler, *J. Am. Chem. Soc.*, **98**, 4342 (1976).
(15) F. B. Kaufman, E. M. Engler, D. C. Green, and J. Q. Chambers, *J. Am. Chem. Soc.*, **98**, 1596 (1976).
(16) G. T. Pott and J. Kommandeur, *Mol. Phys.*, **13**, 373 (1967).
(17) S. J. La Placa, to be published.
(18) B. Welber, *Rev. Sci. Instrum.*, **47**, 183 (1976).
(19) (a) C. K. Johnson, C. R. Watson, and R. J. Warmack, *Am. Cryst. Assoc., Meeting Abstr.* **3**, 19 (1975); (b) C. K. Johnson and C. R. Watson, *J. Chem. Phys.*, **64**, 2271 (1976); (c) F. Wudl, *J. Am. Chem. Soc.*, **97**, 1962 (1975).
(20) J. Q. Chambers, D. C. Green, F. B. Kaufman, E. M. Engler, B. A. Scott, and R. R. Schumaker, *Anal. Chem.*, **49**, 802 (1977).
(21) D. J. Dahm, G. R. Johnson, F. L. May, M. G. Miles, and J. D. Wilson, *Cryst. Struct. Commun.*, **4**, 673 (1975).
(22) A preliminary indexing of our $(TTF)Cl_{0.9}$ pattern on the basis of a tetragonal cell gave $a = 13.97$ Å, $c_0 = 16.4$ Å; however, the pattern could not be completely indexed with these parameters, and structural information will have to await isolation of single crystals.
(23) D. J. Dahm, personal communication.
(24) S. Hunig, G. Kiesslich, H. Quast, and D. Schentzow, *Justus Liebigs Ann. Chem.*, **766**, 310 (1973).
(25) J. B. Torrance, Proceedings of the Conference on Organic Conductors and Semiconductors, Siofok, Hungary, Aug 1976.
(26) J. B. Torrance and B. D. Silverman, *Phys. Rev. B*, **15**, 788 (1977). Note that in this paper the stoichiometry range for the ordered $(TTF)Br_\rho$ phase is taken to be that inferred from x-ray measurements ($0.74 \leq \rho \leq 0.79$), rather than the chemically analyzed range $0.71 \leq \rho \leq 0.76$.
(27) R. M. Metzger and A. N. Bloch, *J. Chem. Phys.*, **63**, 5098 (1975).
(28) M. Born and K. Huang, "Dynamical Theory of Crystal Lattices", Oxford University Press, London, 1954.
(29) R. Gleiter, E. Schmidt, D. O. Cowan, and J. P. Ferraris, *J. Electron Spectrosc. Relat. Phenom.*, **2**, 207 (1973).
(30) L. Pauling, "The Nature of the Chemical Bond", Cornell University Press, Ithaca, N.Y., 1960, p 511.
(31) B. D. Silverman, W. D. Grobman, and J. B. Torrance, *Chem. Phys. Lett.*, in press.
(32) J. B. Torrance and B. D. Silverman, *Bull. Am. Phys. Soc.*, **20**, 498 (1975).
(33) (a) W. D. Grobman, R. A. Pollak, D. E. Eastman, E. T. Maas, Jr., and B. A. Scott, *Phys. Rev. Lett.*, **32**, 534 (1974); (b) W. D. Grobman, and B. D. Silverman, *Solid State Commun.*, **19**, 319 (1976); (c) W. D. Grobman and E. Koch, "Photoemission from Organic Molecular Crystals", in "Topics in Applied Physics", M. Cardona and L. Ley, Ed., Springer, Heidelberg, 1977.
(34) (a) A. J. Epstein, N. O. Lipari, P. Nielson, and D. J. Sandman, *Phys. Rev. Lett.*, **34**, 914 (1975); (b) J. J. Ritsko, N. O. Lipari, P. C. Gibbons, and S. E. Schnatterly, *Bull. Am. Phys. Soc.*, **21**, 311 (1976).
(35) (a) F. Denoyer, R. Comès, A. F. Garito, and A. J. Heeger, *Phys. Rev. Lett.*, **35**, 445 (1975); (b) S. Kagoshima, H. Anzai, K. Kajimura, and T. Ishiguro, *J. Phys. Soc. Jpn.*, **39**, 1143 (1975).
(36) (a) H. A. Mook, and C. R. Watson, Jr., *Phys. Rev. Lett.*, **36**, 801 (1976); (b) R. Comès, S. M. Shapiro, G. Shirane, A. F. Garito, and A. J. Heeger, *ibid.*, **35**, 1518 (1975).
(37) F. H. Herbstein in "Perspectives in Structural Chemistry", J. D. Dunitz and J. A. Ibers, Ed., Wiley, New York, N.Y., 1971, p 166.
(38) B. D. Silverman, *Phys. Rev. B*, submitted.
(39) I. S. Gradshteyn and I. M. Ryzhik, "Table of Integrals, Series and Products", Academic Press, New York, N.Y., 1966.

Crystal and Molecular Structure of the Free Base Porphyrin, Protoporphyrin IX Dimethyl Ester

Winslow S. Caughey[1] and James A. Ibers*[2]

Contribution from the Department of Biochemistry, Colorado State University, Fort Collins, Colorado 80523, and Department of Chemistry, Northwestern University, Evanston, Illinois 60201. *Received March 23, 1977*

Abstract: The structure of the free base porphyrin, protoporphyrin IX dimethyl ester, has been determined from three-dimensional x-ray diffraction data collected from a crystal of calculated weight 0.98 μg. The porphyrin crystallizes with two molecules per unit cell in the triclinic space group C_i^1-$P\bar{1}$ with $a = 11.303$ (5), $b = 22.553$ (10), $c = 6.079$ (3) Å, $\alpha = 91.38$ (2), $\beta = 94.08$ (2), $\gamma = 81.96$ (1)°, $V = 1530$ Å^3. The structure has been refined anisotropically by full-matrix least-squares methods to a final unweighted R index (on F^2) of 0.108 for 397 variables and 3889 observations. The R index (on F) for the 1982 observations having $F_o^2 \geq 3\sigma(F_o^2)$ is 0.073. Bond lengths and bond angles within the porphyrin core have been determined to estimated standard deviations of ±0.006 Å and ±0.5°. The structural results for the porphyrin core do not differ significantly from those found in the free base porphyrin, mesoporphyrin IX dimethyl ester. In the present structure the vinyl groups approach planarity with the porphyrin core more than do the ethyl groups in mesoporphyrin IX dimethyl ester, but these vinyl groups fail to achieve coplanarity owing to steric constraints. The replacement of vinyl groups with ethyl groups results in some significant changes in spectral properties, in the basicity of amide nitrogen atoms, and in the binding of ligands to a central metal without causing a detectable change in the stereochemistry of the porphyrin ring.

The asymmetric pattern of substitution of the naturally occurring porphyrins is manifested in a number of spectroscopic effects. Whether or not the substitution pattern affects the metrical details of such porphyrins, particularly of the inner core, has not been assessed owing to the lack of data on the structures of free base porphyrins. Earlier we reported the structure of the free base porphyrin, mesoporphyrin IX dimethyl ester (MPIX DME).[3] Here we describe the structure of the free base porphyrin, protoporphyrin IX dimethyl ester (PPIX DME). The structural similarities of these two porphyrins are contrasted with their spectral differences.

Experimental Section

Protoporphyrin IX dimethyl ester was obtained from bovine blood hemin chloride, the chloroiron(III) species with unesterified propionic acid groups, via a procedure described earlier.[4] This procedure permits the iron removal and esterifications to be carried out in a single step within a mixture of the hemin, HCl, methanol, chloroform, and ferrous acetate. Crystals were obtained by the diffusion of methanol into chloroform solutions of the porphyrin at 8 °C over a 5-month period. Crystals so obtained were exceedingly small.

Preliminary Weissenberg and precession photographs taken with Cu Kα radiation showed only the required center of symmetry; hence,